Appl. Phys. B (2015) 118:75–83
DOI 10.1007/s00340-014-5956-1

Applied Physics B
Lasers and Optics

Wavelength modulation spectroscopy with signal–reference beam method for highly sensitive gas detection

Wei Wei · Jun Chang · Qingjie Huang · Cunguang Zhu · Qiang Wang · Zongliang Wang · Guangping Lv

Received: 26 March 2014 / Accepted: 28 October 2014 / Published online: 5 November 2014

Abstract Wavelength modulation spectroscopy combined with signal–reference beam method is used for trace gas detection. The developed technique combines the advantages of common-mode noise suppression and signal-to-noise ratio improvement. The performance of the resulting water vapor sensor is markedly improved because of scanning baseline suppression, effective suppression of the target gas content in the components and resistance to external factors such as temperature and humidity. Trace water vapor detection experiments verify that the measurement accuracy of the system can reach 1 ppmv for an optical path length of 10 cm.

W. Wei · J. Chang (✉) · Q. Huang · C. Zhu · Q. Wang · Z. Wang · G. Lv
School of Information Science and Engineering and Shandong Provincial Key Laboratory of Laser Technology and Application, Shandong University, Jinan 250100, China
e-mail: changjun@sdu.edu.cn

W. Wei
e-mail: zero931103056@126.com

Q. Huang
e-mail: qjhuang@sdu.edu.cn

C. Zhu
e-mail: 2003410572@163.com

Q. Wang
e-mail: 1483163606@qq.com

Z. Wang
e-mail: 330121816@qq.com

G. Lv
e-mail: pingping@sdu.edu.cn

1 Introduction

Tunable diode laser absorption spectroscopy (TDLAS) has been widely used to determine gas concentration [1–4]. The laser diodes (LDs) used in TDLAS possess the benefits of being compact and stable and allowing temperature control [5]. Compared with other conventional gas-sensing methods that involve intermittent or continuous sample extraction, in situ measurement provides real-time data without the problems of inherent time delay, blockages in the sampling tube and secondary reactions during gas transport. As lasers become cheaper and more available with the development of the optical industry, TDLAS in the near-infrared (NIR) region becomes more attractive.

Wavelength modulation spectroscopy (WMS) is based on the modulation of the light emitted by a LD that is slowly tuned across an absorption line of the species to be detected. The signal of the second harmonic is proportional to the concentration of the gas species and can be measured with a lock-in amplifier (LIA). An important advantage of this technique is that it shifts the detection to higher frequencies, where the laser excess noise (1/f noise) becomes negligible. As a result, WMS is one to two orders of magnitude more sensitive than direct detection [6–8].

Because it suppresses common-mode effects, signal–reference beam method has long been used for gas detection. This method uses signal and reference beams [9], subtracting, dividing and balanced ratio metric detection circuit. The signal beam propagates through the gas cell to detect gas concentration. Meanwhile, the reference beam propagates through the same optical path length. External factors such as temperature, humidity and fiber fluctuation can then be suppressed by subtraction. In particular, the effect of detected gas contained in components of the system,

which could seriously influence accuracy and resolution, can be avoided.

We have developed a measurement system based on TDLAS for high-sensitivity measurement of water vapor. This optical fiber gas sensor combines signal–reference beam method and WMS and is validated using a 1,370-nm LD.

2 Experiment setup and detection theory

Our system for trace measurement of water vapor used a distributed feedback laser diode (DFB-LD; WSLS-137010C1424-20; Aoshow, CHN) with an emission wavelength of 1,370 nm as the light source. The experimental setup is shown in Fig. 1. In the NIR region, spectral line width of the DFB-LD is very narrow. It is difficult to keep the optical wavelength of the LD at line center because of the fluctuation of outside temperature and the slight drift of the oscillation current. The wavelength-sweep technique and WMS were used to detect the absorption line with a low-frequency scanning signal and high-frequency sine modulation signal, respectively, as the laser drive current. An overlapped mixed signal containing a 1.42-KHz sinusoidal modulation signal and 7.8-Hz trapezoidal scanning signal for the DFB-LD (Fig. 1a) was generated by an ARM7 processor (LTC1758, NXP, the Netherlands). To prevent phase difference generation while demodulating, a 2.84-KHz square wave reference signal (Fig. 1b) was synchronously generated by the same signal source.

The LD radiation was then coupled into a 3-dB coupler and split into two parts. One part, called the signal beam, passed through a gas cell with a path length of 10 cm. With the absorption information of the gas cell and light path, the signal beam irradiated onto an InGaAs photodiode (PD) with a responsivity of 0.8 A/W, as shown in Fig. 1c. The other part of the radiation, called the reference beam, which only contained information about the light path (Fig. 1d), was directly coupled with an identical InGaAs PD. After subtraction of the reference beam from the signal beam, the scanning baseline, external disturbance and the effect of gas contained in the light path was suppressed, as shown in Fig. 1e. The subtraction output was connected to a LIA as an input. With the help of the reference signal generated by the ARM7, the LIA-demodulated input signal was produced, as depicted in Fig. 1f. Finally, the result from the LIA was sent back to ARM7 or to a computer for collection and processing.

TDLAS with WMS mostly detects the 2f signal with modulation index $m = 2.2$ to maximize the signal-to-noise ratio (SNR). For small m ($\ll 1$), we usually use a simpler analysis based on the Taylor-series expansion of the absorption line [10, 11]. For large m, Fourier decomposition of the absorption line function has been applied [12, 13].

Once the monochromatic radiation of the light source overlaps with a rotation/vibration transition of a gas species, absorption will occur, resulting in the attenuation of light intensity. The transmitted intensity $I_{\text{out}}(t)$ at simultaneous time t associated with a rotation/vibration transition in a gas cell is given by the Beer–Lambert law:

$$I_{\text{out}}(t) = I_{\text{in}} \cdot \exp\{-\alpha[\nu(t)]CL\} \tag{1}$$

where I_{in} is incident intensity, $\alpha[\nu(t)]$ (cm^{-1}) is absorption coefficient at instantaneous frequency $\nu(t)$, L(cm) is the optical path length through which the laser beam and gas molecules interact, and C is the mole fraction of the absorbing species in the mixed gas (i.e., target gas density ratio in the mixed gas) in the gas cell and light path. In the case of low-concentration detection, approximation is valid for weak absorbance, i.e., $\alpha[\nu(t)]CL \ll 1$, which can be written as:

$$I_{\text{out}}(t) = I_{\text{in}} \cdot \exp\{-\alpha[\nu(t)]CL\} \approx I_{\text{in}} \cdot \{1 - \alpha[\nu(t)]CL\} \tag{2}$$

For a gas absorption line under regular pressure and temperature, the Lorentzian line-shape function is adopted:

$$\alpha[\nu(t)] = \frac{\alpha_0}{1 + \left[\frac{\nu(t)-\nu_0}{\gamma}\right]^2} \tag{3}$$

where α_0 and ν_0 are frequency and absorption coefficient at the absorption line center, respectively, and γ is half of the line width.

Other than wavelength modulation (WM) for tunable LDs, the drive current signals applied to it produce an increase in laser power as the trapezoid current level increases and its sinusoidal modulation, which is known as amplitude modulation (AM). Then, simultaneous frequency $\nu(t)$ and incident intensity can be written as [14]:

$$\nu(t) = \overline{\nu} + \Delta\nu \cdot \cos\omega t \tag{4}$$

$$I_{\text{in}}(t) = \overline{I}_{\text{in}} + \Delta I \cdot \cos\omega t \tag{5}$$

where average quantities $\overline{\nu}$ and $\overline{I}_{\text{in}}$ are varied slowly relative to angular frequency ω as the laser is scanned across the absorption features. $\Delta\nu$ is the amplitude of WM, and ΔI is the amplitude of sinusoidal intensity modulation, which is determined from the slope of a plot of laser power *versus* current. This allows Eq. (2) to be rewritten as:

$$I_{\text{out}}(t) = (\overline{I}_{\text{in}} + \Delta I \cdot \cos\omega t) \cdot \{1 - \alpha[\nu(t)]CL\} \tag{6}$$

Because the signal and reference beams are set and a subtraction process is applied after photoelectric conversion of the two beams, equivalent laser intensity $I_{\text{out}}(t)$ coupled on the PD will be:

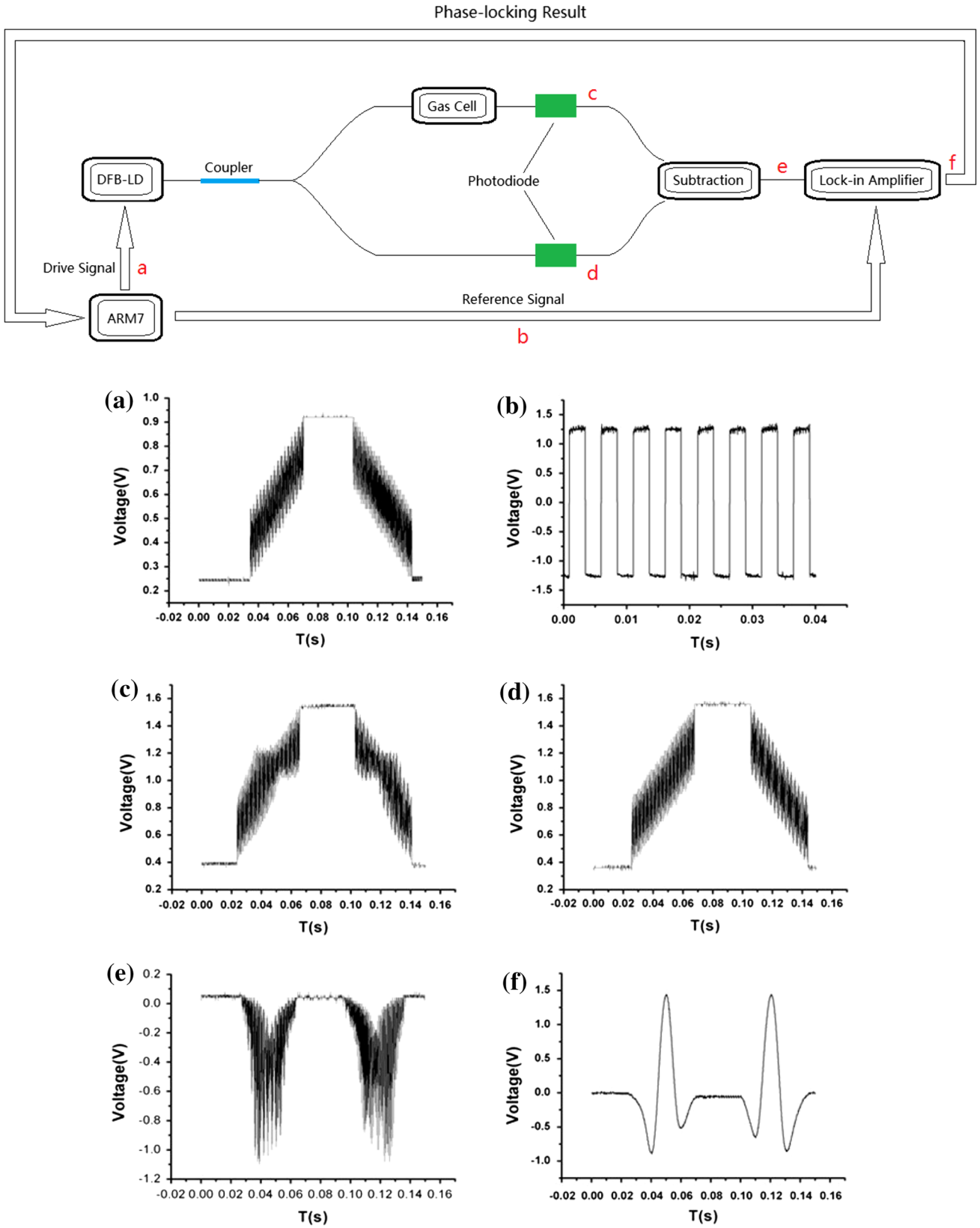

Fig. 1 Experimental configuration. **a** Drive signal, **b** reference signal, **c** output of signal beam, **d** output of reference beam, **e** output of subtractor and amplifier, **f** output of lock-in amplifier

$$I_{\text{outdif}}(t) = (\bar{I}_{\text{in}} + \Delta I \cdot \cos \omega t) \cdot \{1 - \alpha[\nu(t)]CL\} - (\bar{I}_{\text{in}} + \Delta I \cdot \cos \omega t) \cdot \{1 - \alpha[\nu(t)]C'L\} = (\bar{I}_{\text{in}} + \Delta I \cdot \cos \omega t) \cdot \{-\alpha[\nu(t)] \cdot (C - C')L\} \quad (7)$$

where C' is the mole fraction of the absorbing species in the light path. By developing the function in a Fourier cosine series, full expression of laser intensity $I_{\text{outdif}}(t)$ is obtained:

$$I_{\text{outdif}}[\nu(t)] = \left(\bar{I}_{\text{in}} + \Delta I \cdot \cos \omega t\right) \cdot \sum_{k=0}^{k=+\infty} H_k(\bar{\nu}, \Delta\nu) \cos(k\omega t) \quad (8)$$

For convenience, $\omega \bullet t$ is substituted by u during the following calculations, and functions $H_k(\bar{\nu}, \Delta\nu)$ are given by:

$$H_0(\bar{\nu}, \Delta\nu) = \frac{1}{2\pi} \int_{-\pi}^{+\pi} \left[-\alpha(\bar{\nu} + \Delta\nu \cdot \cos u) \cdot (C - C')L\right] \mathrm{d}u \quad (9)$$

$$H_k(\bar{\nu}, \Delta\nu) = \frac{1}{\pi} \int_{-\pi}^{+\pi} \left[[-\alpha(\bar{\nu} + \Delta\nu \cdot \cos u) \cdot (C - C')L\right] \cdot \cos ku \mathrm{d}u \quad k > 0 \quad (10)$$

Then, the final expression for the second-harmonic signal (2f signal) S_2 is:

$$S_2(\bar{\nu}) = -\frac{\Delta I}{2} H_3(\bar{\nu}, \Delta\nu) + \bar{I}_{\text{in}} H_2(\bar{\nu}, \Delta\nu) - \frac{\Delta I}{2} H_1(\bar{\nu}, \Delta\nu) \quad (11)$$

The second Fourier component H_2 contributes the most to 2f signal S_2. However, AM is responsible for the distortion of the signal compared with the case of pure wavelength modulation, as shown by the presence of ΔI in Eq. (11). At the same time, second-harmonic signal expression of single-beam WMS [i.e., Eq. (6)] resembles that of signal–reference beam method [i.e., Eq. (7)].

3 Results

In our experiment, we used the absorption line center at 1,368.597 nm, which was the highest absorption point within the spectral range of the DFB-LD. A water meter (S8000, Integrale Precision Dewpointmeter, Michell, UK) was used to calibrate water concentration. All experiments were performed at a temperature of 24 ± 1 °C every 10 min, humidity of 23 % and concentration of water vapor between 30 and 1,100 ppmv.

Because there was large amount of water vapor in the light path, the measured results were modified using a water vapor detection system. The graphs in Fig. 2 are results after modification for the equivalent content of water vapor contained in the system, while the insets depict results before modification. The relationships between measured results and the calibration of the water meter with only the signal–reference beam method and only WMS are presented in Fig. 2a, b, respectively. Measurement accuracies in Fig. 2a, b are 18 and 10 ppmv, respectively, which were determined by comparing measured and calibration results.

Figure 2c depicts the relationship between measured results and the calibration of the water meter for the combined system using both signal–reference beam method and WMS. Because factors such as scanning baseline, target gas contained in the components and environmental influences are suppressed, the accuracy of the combined system is 1 ppmv.

3.1 Scanning baseline

The wavelength-sweep technique was used because it was difficult for the wavelength of the laser to remain at the absorption line center (1,368.597 nm), so a low-frequency scanning signal was added to the drive signal of the laser. Empirically, the frequency of a particular profile should be $0.35/\tau_r$, where τ_r is the rise time of the profile [15]. Considering that the frequency of the scanning signal was 7.8 Hz and that the sweep range was 280 pm, τ_r was about 0.02 s and the frequency of the second-harmonic profile was 17.5 Hz. While the frequency of the profile is higher than that of the scanning signal, a low-pass filter cannot effectively filter out the scanning signal. When detecting with a scanning baseline, the profile will be distorted and the quality of the measurement will deteriorate.

The LIA used here was an AD630 (balanced modulator/demodulator, Analog Devices) and its peripheral circuit, including integrator and low-pass filter. When given a 2.84-KHz square wave reference signal, to maximize the SNR without wave distortion, the time constant of the integrator was set as 65 μs and the time constant of the low-pass filter is set as 1.85 ms, which gave a rejection ratio at 7.8 Hz of 42 dB. This resulted in insufficient suppression of low-frequency signals and the scanning baseline remained. Figure 3a shows the profile of the second harmonic with the scanning baseline when the concentration of water vapor in the gas cell is 128 ppmv. The red line is the profile of the second harmonic calculated using Eq. (11) for comparison. Figure 2b shows the relationship between the results measured by the system and the calibration of the water meter. The accuracy of the system is 10 ppmv under these conditions.

Subtraction of the signal converted from the reference beam from that converted from the signal beam is needed to increase the accuracy of the measurement. By adjusting the intensity of light signals and magnification of amplifiers in the circuit, the amplitude of two signals can be equilibrated and the scanning baseline can be suppressed when the concentration of water vapor in gas cell is 128 ppmv (Fig. 3b). The red line is the profile of the second harmonic

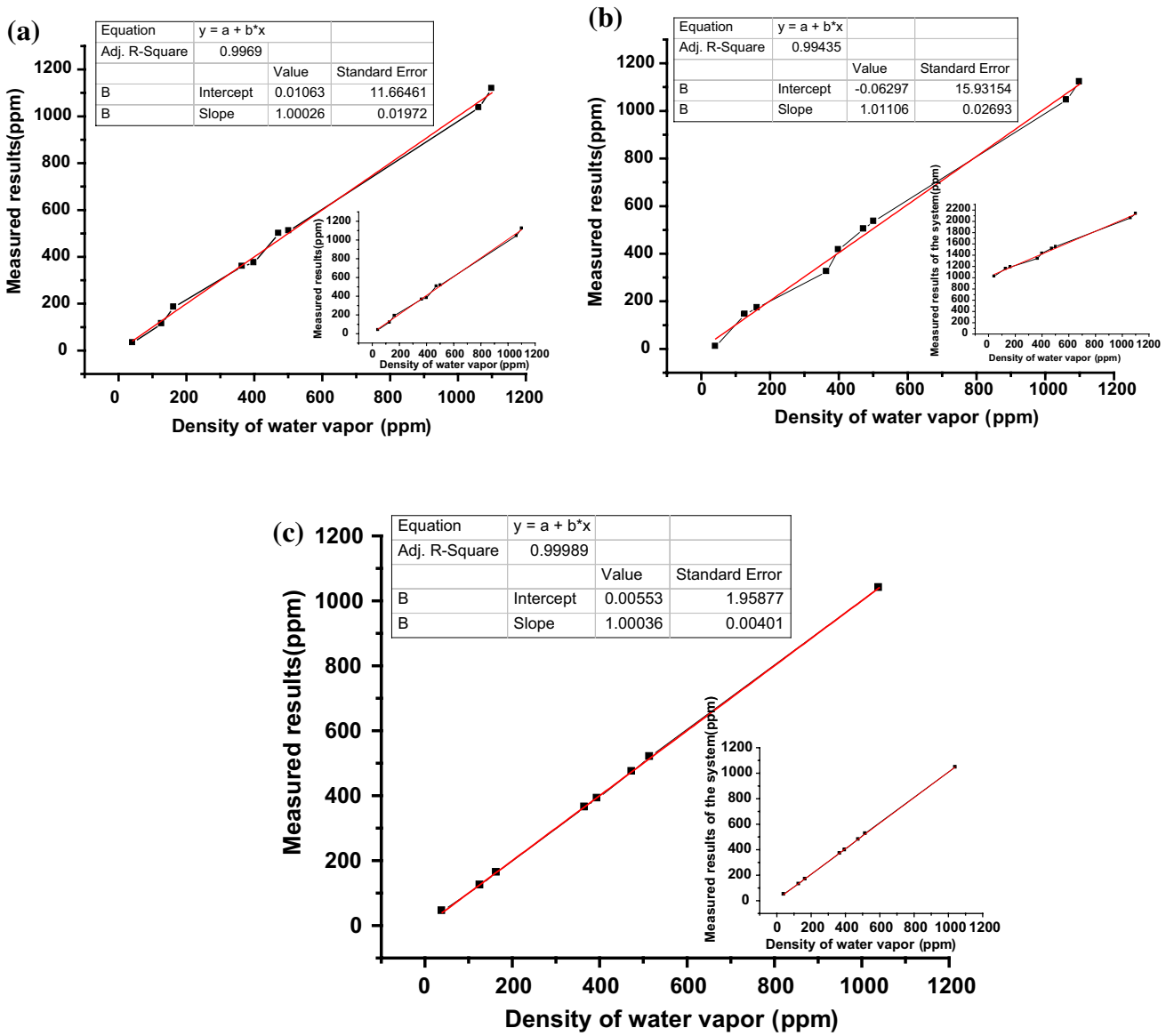

Fig. 2 Measurement linearity of three methods. **a** With signal–reference beam method, **b** with WMS, **c** with signal–reference beam method and WMS

calculated using Eq. (11) for comparison. The scanning baseline can be suppressed by 64 dB using signal–reference beam method and 42 dB using WMS. Therefore, when both signal–reference beam method and WMS are used, the scanning baseline can be suppressed by 106 dB, improving the measured results, as demonstrated above in Fig. 2c.

3.2 Target gas in the components

In trace measurements, the target object contained in the system itself always influences measurements, and this is especially the case in trace gas measurements. Firstly, target gas contained in components will reduce the measurement range of the acquisition section. For example, the ARM7 (LTC1758) used here contained a single 12-bit successive approximation analog-to-digital converter (ADC) and had a working voltage range of 0–3.0 V and resolution of 0.73 mV. When the concentration of water vapor changes between 30 and 1,100 ppmv, the theoretical resolution of the system is 0.27 ppmv. In practice, the content of water vapor in the light path, which includes the DFB-LD, PD and fiber, exceeds 1,000 ppmv when the optical path length is 10 cm. In this case, the theoretical resolution will be 0.66 ppmv. Limited by the sensitivity of the PD, the actual resolution is 1.6 ppmv. Secondly, the content of target gas in the components depends on environment [16, 17].

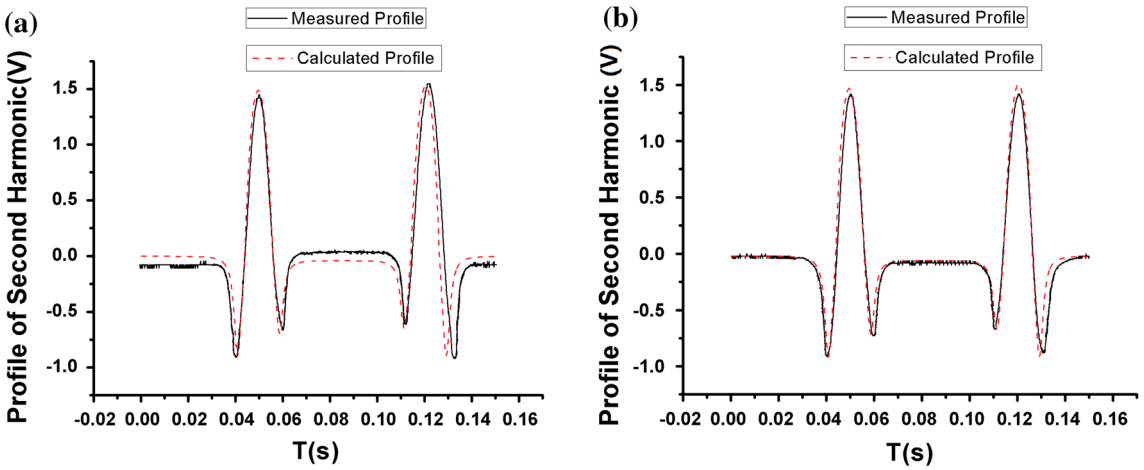

Fig. 3 Profiles for water vapor measured. **a** With the scanning baseline, **b** with the scanning baseline suppressed

Table 1 Effect of light intensity loss on measured results with 40 ppmv water vapor in the gas cell and 1,000 ppmv in components

Intensity attenuation (%)	Error from modification (ppmv)	Error from subtraction and modification (ppmv)
2	3	1
5	4	2
10	6	3
15	15	8

Signal–reference beam method can reduce the equivalent content of water vapor in the system. Equation 6 and 7 show that the equivalent water vapor contained in single-beam WMS would be C (i.e., the mole fraction of the absorbing species in the gas cell and light path), while that in a combination of signal–reference beam method and WMS would be $C–C'$ (i.e., mole fraction of the absorbing species in the gas cell and difference of the light paths). As long as the PDs in the two paths are of the same type and in an identical environment, the difference of water vapor content in the PDs approaches zero, so equivalent content of water vapor contained in the light path would be very small. This value is about 8 ppmv in experiments. When the full working range of the ADC is used and equivalent content fluctuation caused by environmental change is minimized, the resolution of the systems is improved to 0.4 ppmv and accuracy is improved to 1 ppmv.

3.3 External influences

External influences such as temperature, humidity and fiber vibration affect the stability and accuracy of the optical measurement system. Fiber vibration will attenuate the light intensity that propagates to the PD. We can suppress this effect by modifying the measured results. By measuring second-harmonic amplitude with light intensity changes at the same concentration, we can determine the relationship between light intensity and second-harmonic amplitude. The detected results can then be modified using this relationship, especially when light intensity varies. However, suppressing light intensity attenuation by using signal–reference beam method before modification is more effective. For detection under conditions where the water vapor contained in the components of the system is about 1,000 ppmv and the actual water vapor in the gas cell is 40 ppmv, the measured errors caused by light intensity attenuation for modification and modification after signal–reference signals subtraction are listed in Table 1. The greater the intensity attenuation, the smaller the error caused by subtraction before modification compared with that for modification alone.

The output power of DFB-LDs increases with temperature [18]. In addition, the content of vapor in components will change with temperature. Changes in humidity also influence the concentration of vapor in the components of the system. As discussed above, the equivalent water vapor contained in the signal–reference beam method and WMS would be $C–C'$. As long as the PDs in the two paths are of the same type and in identical environments, the influence of temperature or humidity changes on the two light paths should be very similar and the difference between them approaches zero. As a result, signal–reference beam method can effectively suppress changes induced by fluctuations in temperature and humidity.

To test the resistance of the measurement system to temperature fluctuation, the surrounding temperature was set to change within the scope of 8 °C around 24 °C every 10 min. Figure 4 shows the relationships between

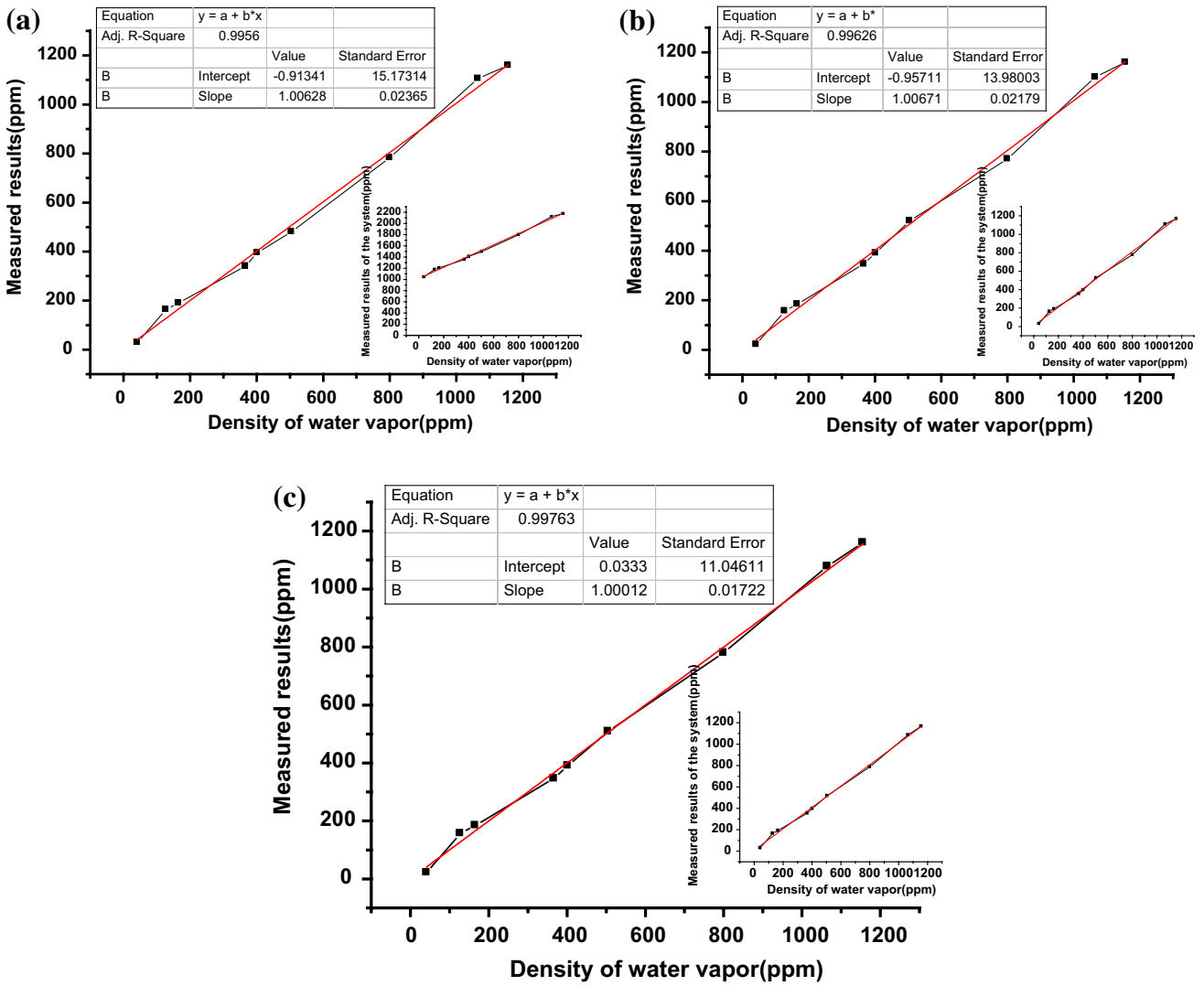

Fig. 4 Dependence of measurement results on temperature fluctuation. **a** With WMS, **b** with signal–reference beam method, **c** with signal–reference beam method and WMS

the results obtained using the system and the calibration of the water meter with the methods of only WMS, only signal–reference beam method and both signal–reference beam method and WMS. The effect of temperature on measured results with only WMS and only signal–reference beam method was 21 and 9 ppmv, respectively. The influence of temperature is suppressed by 4 ppmv using a combination of signal–reference beam method and WMS.

To test the resistance of the measurement system to humidity fluctuation, the surrounding humidity was set to change between 25 and 21 % every half hour. Figure 5 illustrates the relationships between results measured using our system and the calibration of the water meter with the methods of only WMS, only signal–reference beam method and the combination of signal–reference beam method and WMS. The influence of humidity on measured results with only WMS and only signal–reference beam method was 12 and 7 ppmv, respectively. The effect of humidity is decreased by 3 ppmv with the combination of signal–reference beam method and WMS. Table 2 summarizes the resistance to temperature and humidity fluctuation for the system using different methods.

4 Conclusion

The advantages of signal–reference beam method and WMS can be obtained at the same time by using a combination of these methods. Using both methods can suppress the effects of scanning baseline residues, detected gas contained in the components and external influences such as

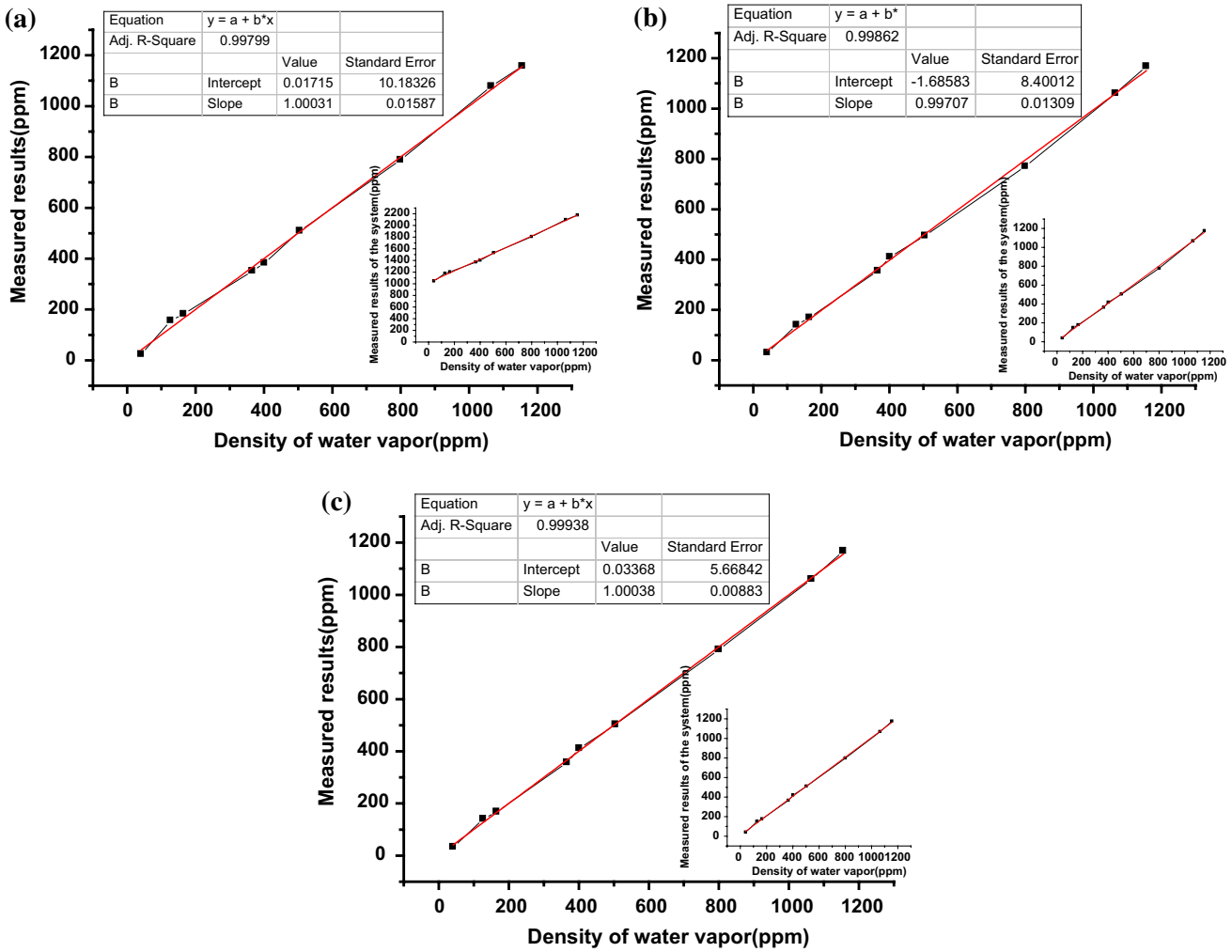

Fig. 5 Effect of humidity changes on measured results. **a** With WMS, **b** with signal–reference beam method, **c** with signal–reference beam method and WMS

Table 2 Measurement accuracy of three methods under different conditions

	Measurement accuracy (T: 24 ± 0.5 °C, H: 23 %)	Measurement accuracy (T: 24 ± 4 °C, H: 23 %)	Measurement accuracy (T: 24 ± 0.5 °C, H: 23 ± 2 %)
With WMS	10	31	22
With signal–reference beam method	18	27	25
With signal–reference beam method and WMS	1	5	4

temperature and humidity, improving the accuracy of water vapor detection to 1 ppmv.

To optimize SNR without wave distortion, the time constant of the integrator and low-pass filter was set as 65 μs and 1.85 ms, respectively. Because of insufficient suppression of low-frequency signals, the scanning baseline will remain and accuracy will be affected. Compared with single-beam WMS, WMS after signal–reference beam method suppressed the scanning baseline to 106 dB, increasing the accuracy of the measured results.

Signal–reference beam method decreased the equivalent content of detected gas in the components and suppressed its influence on the system. In our experiment, water vapor contained in the laser and PD was over 1,000 ppmv for an

optical path length of 10 cm. After signal–reference beam method, the equivalent content of water vapor decreases to about 8 ppmv, which improves the resolution from 1.6 to 0.4 ppmv.

Subtraction of the reference beam from the signal could suppress most changes caused by external factors. In our experiment, the effects of temperature variation, humidity variation and output power fluctuation on the measured results were suppressed markedly. When temperature fluctuated by 8 °C around 24 °C, the effect of temperature on experiment results was suppressed by 4 ppmv, and when atmospheric humidity changed between 25 and 21 %,the influence of humidity was suppressed by 3 ppmv.

Acknowledgments This work was supported by National Natural Science Foundation of China (60977058&61475085), Science and technology development project of Shandong province (2014GGX101007), The Fundamental Research Funds of Shandong University (2014YQ011).

References

1. M.A. Bolshov, Y.A. Kuritsyn, V.V. Liger, V.R. Mironenko, S.B. Leonov, D.A. Yarantsev, Measurements of the temperature and water vapor concentration in a hot zone by tunable diode laser absorption spectrometry. Appl. Phys. B Lasers Opt. **100**, 397–407 (2010)
2. S. Hunsmann, K. Wunderle, S. Wagner, U. Rascher, U. Schurr, V. Ebert, Absolute, high resolution water transpiration rate measurements on single plant leaves via tunable diode laser absorption spectroscopy (TDLAS) at 1.37 μm. Appl. Phys. B Lasers Opt. **92**, 393–401 (2008)
3. G. Durry, J.S. Li, I. Vinogradov, A. Titov, L. Joly, J. Cousin, T. Decarpenterie, N. Amarouche, X. Liu, B. Parvitte, O. Korablev, M. Gerasimov, V. Zéninari, Near infrared diode laser spectroscopy of C_2H_2, H_2O, CO_2 and their isotopologues and the application to TDLAS, a tunable diode laser spectrometer for the martian PHOBOS-GRUNT space mission. Appl. Phys. B Lasers Opt. **99**, 339–351 (2010)
4. Q. Wang, J. Chang, C.-G. Zhu, C. Li, F.-J. Song, Y.-N. Liu, X.-Z. Liu, Detection of water vapor concentration based on difference value of two adjacent absorption peaks. Laser Phys. Lett. **9**(6), 421–425 (2012)
5. F. Wang, K.F. Cen, N. Li, Q.X. Huang, X. Chao, J.H. Yan, Y. Chi, Simultaneous measurement on gas concentration and particle mass concentration by tunable diode laser. Flow Meas. Instrum. **21**, 382–387 (2010)
6. X. Wang et al., Measurement of CO_2 concentration in flame based on tunable diode laser absorption spectroscopy. J. Atmos. Environ. Opt. **2**(4), 290–295 (2007)
7. J. Cao, K. Zhang, R. Yang, Z. Wang, in *Modulation Coefficient Analysis in Optical Fiber Methane Gas Sensor Based on Wavelength Modulation Spectroscopy*. World Congress on Intelligent Control and Automation, 6–9 July 2010, Jinan, China
8. K. Duffin, A.J. McGettrick, W. Johnstone, G. Stewart, D.G. Moodie, Tunable diode-laser spectroscopy with wavelength modulation: a calibration-free approach to the recovery of absolute gas absorption line shapes. J. Lightwave Technol. **25**(10), 3114–3125 (2007)
9. Q. Wang, J. Chang, C. Zhu, Y. Liu, G. Lv, F. Wang, X. Liu, Z. Wang, High-sensitive measurement of water vapor: shot-noise level performance via a noise canceller. Appl. Opt. **52**(5), 1094–1099 (2013)
10. O.E. Myers, E.J. Putzer, Measurement broadening in magnetic resonance. J. Appl. Phys. **30**(12), 1891–1897 (1959)
11. A.M. Russel, D.A. Torrchia, Harmonic analysis in systems using phase sensitive detectors. Rev. Sci. Instrum. **33**(12), 442–444 (1962)
12. J. Reid, D. Labrie, Second-harmonic detection with tunable diode lasers—comparison of experiment and theory. Appl. Phys. B Lasers Opt. **26**(3), 203–210 (1981)
13. J.M. Supplee, A. Whittaker, W. Lenth, Theoretical description of frequency modulation and wavelength modulation spectroscopy. Appl. Opt. **33**(27), 6294–6302 (1994)
14. L.C. Philippe, R.K. Hanson, Laser diode wavelength-modulation spectroscopy for simultaneous measurement of temperature, pressure and velocity in shock-heated oxygen flows. Appl. Opt. **32**(30), 6090–6103 (1993)
15. Q. Wang, J. Chang, Z. Wang, C. Tian, S. Jiang, G. Lv, Study of an optical fiber water vapor sensor based on a DFB diode laser: combined wavelength scanning and intensity modulation. J. Mod. Opt. **61**(18), 1538–1544 (2014)
16. Qiang Wang, Jun Chang, Fujun Song, Fupeng Wang, Cunguang Zhu, Zhi Liu, Sasa Zhang, Xiangzhi Liu, Measurement and analysis of water vapor inside optical components for optical fiber H_2O sensing system. Appl. Opt. **52**, 6445–6451 (2013)
17. C.G. Zhu, J. Chang, P.P. Wang, B.N. Sun, Q. Wang, W. Wei, X.Z. Liu, S.S. Zhang, Improvement of measurement accuracy of infrared moisture meter by considering the impact of moisture inside optical components. IEEE Sens. J. **14**, 920–925 (2014)
18. C. Zhu, J. Chang, P. Wang, W. Wang, Q. Wang, Y. Liu, G. Lv, X. Liu, W. Wei, F. Wang, S. Zhang, Reliability analysis and comparison of demodulation methods for dual-beam wavelength-modulation spectroscopy water vapor detection. Appl. Opt. **52**(18), 4171–4178 (2013)